Journal of Physics: Conference Series **547** (2014) 012006 doi:10.1088/1742-6596/547/1/012006

Analysis of thermodynamic losses in ground source heat pumps and their influence on overall system performance

C Casarosa, P Conti, A Franco, W Grassi, D Testi

Department of Energy, Systems, Territory and Constructions Engineering (DESTEC), University of Pisa, Largo Lucio Lazzarino – 56122 Pisa, Italy

E-mail: paolo.conti@for.unipi.it

Abstract. The present work aims at identifying the relative influence of GSHP subsystems (viz. ground source, earth heat exchangers, heat pump unit, pumping devices) on the overall efficiency and the limits to which technological improvements should be pushed (because, beyond these limits, only minor benefits may be achieved). To this end, an analysis of thermodynamic losses is conducted for a case study, followed by a sensitivity analysis on the heat pump unit thermal performance. Primary energy consumptions of nine configurations with different combinations of ideal and real subsystems are compared. The completely ideal system is used as the reference to normalize energy consumptions and obtain a dimensionless efficiency parameter. The results show that – when a proper design methodology is employed – the performance of the borehole heat exchangers slightly affects the overall efficiency. On the contrary, the thermal response of the ground and the thermal and hydraulic performances of the heat pump unit are key factors. Finally, a sensitivity analysis is conducted by increasing the heating and cooling efficiencies of the heat pump device.

1. Introduction

Ground source heat pump (GSHP) systems are globally recognized as one of the most promising technologies in terms of economic and energy savings. However, despite the aroused interest, operative performances can be lower than expected [1–4], possibly reducing the attractiveness of GSHPs with respect to air heat pumps and condensing boilers.

As well known, GSHPs involve different subsystems: ground source, ground-coupled heat exchangers, ground-coupled heat pump unit (GHP), and pumping devices. Remarkable benefits can be achieved through the application of proper sizing and management strategies aimed at optimizing the synergy among GSHP subsystems [5–9]. Further performance enhancement could be obtained by reducing all the possible causes of losses in the system. This work aims to find which component mainly affects the overall performance, in order to evaluate the corresponding room for improvement and – through a sensitivity analysis on technological performances – identify appropriate strategies for GSHP development.

Thermal inefficiencies are typically investigated by means of the "*second-law analysis"* or "*exergy analysis"* (see, for instance, [10]). *Exergy efficiency* (ψ) is the corresponding index of performance: its value, given by the ratio of the desired exergy output to the exergy used, is generally associated with a measure of the relative deviation between a real system and the corresponding ideal one.

Several works have involved exergy analyses of ground heat pumps (see, for instance, [11–15]). However, it is worth recalling that the results of this type of analysis are strongly dependent on the choice of the reference state, especially when the operative temperatures of the system are close to it [12,16]. Heat pump applications are usually investigated using external air as reference state [11–14,17], therefore, this choice is pivotal.

In the present work, an alternative approach has been followed: instead of analyzing exergy fluxes, ideal subsystems are simulated, comparing primary energy consumptions. The GSHP system comprises four subsystems, viz. ground source, borehole heat exchangers (BHEs), ground-coupled heat pump unit (GHP), and pumping devices; each of them has an ideal reference configuration. Combining ideal and real subsystems, nine different configurations, listed in table 1, are obtained.

Table 1. Analyzed configurations in terms of real and ideal subsystems.

Configuration	Ground source	BHEs	GHP	Hydraulic losses
#1	Real	Real	Real	Real
#2	Ideal	Real	Real	Real
#3	Real	Ideal	Real	Real
#4	Real	Real	Ideal	Real
#5	Real	Real	Real	Ideal
#6 = #2 + #4	Ideal	Real	Ideal	Real
#7 = #3 + #4	Real	Ideal	Ideal	Real
#8 = #4 + #5	Real	Real	Ideal	Ideal
#9 = #2 + #3 + #4 + #5	Ideal	Ideal	Ideal	Ideal

Global design and control strategy have been optimized in every configuration, thus, final energy consumptions depend only on the performance of the various subsystems. Considering an ideal subsystem, it is possible to quantify the maximum benefits that can be achieved improving the technological level of each component. The optimization procedure has been presented in [6,7] and it is shortly recalled in Sections 2 and 3.

A dimensionless efficiency parameter (ε) is used to normalize and compare the energetic performances of the different simulated configurations. ε is based on the *"task efficiency"* definition provided by Moran [10]. In the present case, it reads:

$$\varepsilon = \frac{En_p^*}{En_p} \tag{1}$$

Where En_p^* is the theoretical minimum primary energy consumption, obtained by a loss-free system (Configuration #9), and En_p is the actual primary energy consumption of the system.

2. GSHP systems modelling

An introductory scheme for GSHPs simulation has been outlined in [5] and fully developed in [6]. A quasi-steady-state approach is adopted: in each time step, a full set of equations (2), made of each subsystem model, is solved. The two coefficients f_H and f_C represent the control strategy: their value correspond to the fraction of building load delivered by the geothermal heat pump in heating and cooling mode, respectively. The system comprises:

- equation (2.1), which imposes that the total heat exchanged between the BHE field and the ground (Q_g) is equal to the heat transferred in the evaporator/condenser ($Q_{E/C}$);
- equation. (2.2), which is the energy balance for the ground loop in the evaporator/condenser;
- equation (2.3), representing the heat pump unit; the function *F* correlates the HP performance to the operative conditions; in this work, generators performances are evaluated according to the current Italian technical standard [18–20], including the electric energy needed for pumping;
- equation (2.4), representing the BHE field; the function *E* correlates Q_g to the ground temperature at the borehole surface (T_g), to the BHEs characteristics, and to the ground-coupled loop operative parameters (flow rate and temperature); in this work, the classical *ε-NTU* method for heat exchangers analysis has been used;
- equation (2.5), representing the ground source; the function *S* correlates T_g to heat fluxes and thermo-physical properties; in this work, the finite line source model (FLS)[21] has been used together with time and space superposition technique [7,21];
- equation (2.6), which is the share of thermal load at the GHP for heating (f_H) and cooling (f_C);
- equation (2.7), representing the back-up system; similarly to the GHP, the performance of the back-up generator is influenced by its capacity ratio and by the temperature of the end-user loop; the function *B* characterizes the employed back-up technology;
- equation (2.8), which imposes that the building thermal load (Q_l), is given by the sum of the thermal energies delivered/removed by GSHP and back-up generators.

$$\begin{cases} Q_{E/C} = Q_g & (2.1) \\ Q_{E/C} = \dot{m}_w c_w \left| T_{w_{in}} - T_{wout} \right| \tau & (2.2) \\ Q_{E/C} = F\left(T_{w_{in}}, T_l, CR_{H/C}\right) & (2.3) \\ Q_g = E\left(\dot{m}_w, T_{w_{in}}, R_b, H, N_{BHE}\right) & (2.4) \\ T_g = S\left(T_g{}^0, Fo_g, Q_g\right) & (2.5) \\ f_H = \dfrac{Q_E}{Q_l}\left(\dfrac{COP}{COP-1}\right) \quad f_C = \dfrac{Q_C}{Q_l}\left(\dfrac{EER}{EER+1}\right) & (2.6) \\ Q_{E/C} = B\left(T_l, CR_{H/C}\right) & (2.7) \\ Q_{bk} = \left(1 - f_{H/C}\right) \cdot Q_l & (2.8) \end{cases}$$

3. Design and control optimization algorithm

As mentioned in Section 1, both the equipment sizing and control strategy are optimized for each configuration in order to highlight intrinsic inefficiencies. The overall optimization procedure involves two types of control variables: the ones related to the sizing of the earth heat exchangers (viz. number and depth of BHEs and flow rate in the ground-coupled loop) and the ones related to the control strategy (capacity ratio of GHP unit).

The optimization problem was formulated as a "multistage decision problem" [22]. A full discussion on problem formulation and resolution strategy can be found in [7]; here we shortly recall the main aspects. The problem reads:

$$E_p^{tot}(\mathbf{U}) = \min_{\mathbf{U}} \sum_{n=1}^{N} R(\mathbf{u}^n, \mathbf{x}^n) \tag{3}$$

where:

- $\mathbf{u}^n = (u_1{}^n, u_2{}^n, \ldots) = (N_{BHE}, H, \dot{m}_w, CR^n_{H/C})$ is the vector of control variables at the n^{th} stage; design variables have the same value at each stage;
- $\mathbf{x}^n = (x_1{}^n, x_2{}^n, \ldots)$ is the vector of state variables at the n^{th} stage;
- $E_p^{tot}(\mathbf{U})$ is the objective function; in this work, we considered primary energy consumption;
- $\mathbf{U}$ is the set containing all the $\mathbf{u}^n$;
- $R(\mathbf{u}^n, \mathbf{x}^n)$ is the so-called "return function"; it represents the contribution of the n^{th} stage to the total objective function;
- $f(\mathbf{u}^n, \mathbf{x}^n)$ is the mathematical model for GSHP simulation described by set of equations (2); f relates the state variables of a stage to the control and state variables of the previous stage.

The constraints of the optimization variables are:

- the depth of a single borehole (H) cannot exceed 100 m;
- the flow rate ($\dot{m}_w$) in the ducts must be high enough to guarantee a fully turbulent regime ($Re_D > 6000$) and a fluid velocity higher than 0.3 m/s;
- the supply temperature of the ground-coupled loop cannot be lower than 3°C or exceed 35°C, in order to avoid water freezing in the pipes or overheating of the ground.

4. Description of the analyzed configurations

4.1 Configuration #1: Benchmark

The benchmark configuration is based on the test case illustrated in [7]. A ground-coupled vertical heat exchanger heat pump system has been simulated during 10 years of operational life, a convenient period for evaluating the effects of possible long-term ground temperature drifts. The back-up generators are a condensing boiler and an air/water cooler. Heating and cooling loads are imposed, as shown in table 2, according to a numerical example given in [23], referring to a typical medium-scale office in the Mediterranean climate. The characteristics of ground, BHEs and generators employed in the simulation are reported in tables 3 and 4.

4.2 Configuration #2: Ideal ground source

This configuration considers an ideal ground source with an infinite thermal capacity. In this way, BHEs surface temperatures remain always constant: equation (2.e) is replaced by: $T_g^n = T_g^0$.

4.3 Configuration #3: Ideal borehole heat exchangers

In this case, ideal BHEs are employed: borehole thermal resistance (R_b) is considered null and heat exchanger effectiveness is set equal to 1. equation (2.d) is replaced by: $Q_g = \dot{m}_w c_w \left(T_{w_{in}} - T_g\right)\tau$.

4.4 Configuration #4: Ideal ground-coupled heat pump unit

The real GHP unit is replaced by a totally reversible thermodynamic cycle. All the HP components are considered ideal: operating and secondary fluids can exchange heat without temperature difference (no external irreversibilities) and compression and expansion processes are isentropic (no internal irreversibilities). This ideal device can deliver any thermal load without power limitations and with no penalizations due to low capacity ratios ($CR_{H/C}$).

4.5 Configuration #5: Ideal head loss

In this configuration, no distributed or lumped losses are present; thus, pumping energy is null.

Table 2. Monthly heating and cooling loads (GWh) of the tested office building.

	JAN	FEB	MAR	APR	MAY	JUN	JUL	AUG	SEP	OCT	NOV	DEC	**TOT**
Heating demand[a]	16.1	11.7	6.9	1.4	0	0	0	0	0	1.4	8.3	13.9	**59.7**
Cooling demand[b]	0	0	0	0	7.5	14.4	17.2	17.2	6.9	0	0	0	**63.3**

[a] Supply / return temperature of the building end-user loop: 45 / 40 °C.
[b] Supply / return temperature of the building end-user loop: 7 / 12 °C.

Table 3. Ground thermal properties and BHE characteristics.

Property	**Value**
Ground thermal conductivity [W/(m K)]	1.7
Ground thermal diffusivity [mm^2/s]	0.68
BHE diameter [m]	0.15
BHE configuration	Double U
Spacing between boreholes [m]	10
Grouting thermal conductivity [W/(m K)]	1.7
BHE pipe diameter (inner – outer) [m]	0.0262 – 0.032
U shank spacing [m]	0.094
Pipe thermal conductivity [W/(m K)]	0.35
BHE thermal resistance R_b [m K/W]	0.062

Table 4. Declared capacity (DC) of the ground heat pump and back-up generators.

Ground-coupled unit (water/water)		**Condensing boiler**	**Air/water unit**
Heating DC[a]	Cooling DC[b]	Heating DC	Cooling DC[b]
24.7 kW	22.9 kW	33.5 kW	59.2 kW

[a] Outdoor Heat Exchanger: Inlet 0°C / Outlet -3°C; Indoor Heat Exchanger: Inlet 40°C / Outlet 45°C [24].
[b] Outdoor Heat Exchanger: Inlet 30°C / Outlet 35°C; Indoor Heat Exchanger: Inlet 12°C / Outlet 7°C [24].

5. Results and discussion

Optimal control strategies and design variables, together with the main performance indices, are reported for each configuration in tables 5 and 6.

In Configuration #1, the $f_{H/C}$ sequence (control strategy) is given by the optimal synergy among GHP unit and back-up generators (condensing boiler and air/water heat pump). In heating mode, the geothermal solution performs better than the boiler, except during the transitional months (April and October), when the building load is below the control range of the GHP unit. $f_H = 0.9$ in January is due to the constraint imposed on the supply temperature of the ground-coupled loop ($T_{w_{in}} \geq 3$°C): indeed, the optimal BHEs number and depth (7 x 100 m) resulting from the best trade-off between heat transfer performance and pumping energy, is not sufficient to exchange all the heat required to match the building heating load. For the same reasons, during the cooling season, the BHEs field is not able to match the total cooling load, therefore, the air unit integration is always required. Nevertheless, the optimal solution does not split the cooling load between air and ground sources, but it finds more convenient operating the sole air unit during the hottest months (July and August) and the sole GHP during the others (June and September).

In Configuration #2, the ground temperature remains constant; hence, a reduced number of BHEs is sufficient to meet the total heating load.

Table 5. Optimal control strategies.

Configuration	JAN	FEB	MAR	APR	MAY	JUN	JUL	AUG	SEP	OCT	NOV	DEC
#1	0.9	1	1	0	1	1	0	0	1	0	1	1
#2	1	1	1	0	1	1	0.7	0.7	1	0	1	1
#3	1	1	1	0	1	1	0	0	1	0	1	1
#4	0.9	1	1	1	1	1	1	1	1	1	1	1
#5	1	1	1	0	1	1	0.7	0.7	1	0	1	1
#6 = #2 + #4	1	1	1	1	1	1	1	1	1	1	1	1
#7 = #3 + #4	0.9	1	1	1	1	1	1	1	1	1	1	1
#8 = #4 + #5	1	1	1	1	1	1	1	1	1	1	1	1
#9 = #2 + #3 + #4 + #5	1	1	1	1	1	1	1	1	1	1	1	1

Table 6. Optimal design variables and performance indices.

Configuration	E_p^{tot} [MWh]	ε [-]	N_{BHE} [-]	H [m]	$\dot{m}_w$ [kg/s]	f_H [-]	f_C [-]	COP [-]	EER [-]	CR_H [-]	CR_C [-]	η [-]	EER_{air} [-]	CR_{air} [-]
#1	856	0.19	7	100	2.39	0.93	0.46	3.94	3.75	0.98	1	1.09	3.18	0.94
#2	721	0.22	4	100	1.36	0.95	0.84	4.83	4.70	1	0.84	1.09	2.18	0.28
#3	843	0.19	7	100	2.39	0.95	0.46	3.98	3.84	1	1	1.09	3.18	0.94
#4	375	0.42	7	100	2.39	0.97	1	6.41	12.0	0.98	1	1.09	-	-
#5	713	0.22	n.a. (∞)	100	n.a. (∞)	0.95	0.84	5.00	4.67	1	0.84	1.09	2.18	0.28
#6 = #2 + #4	214	0.74	4	100	1.36	1	1	9.08	31.9	1	1		-	-
#7 = #3 + #4	358	0.44	7	100	2.39	0.99	1	6.50	12.7	1	1	1.09	-	-
#8 = #4 + #5	214	0.75	n.a. (∞)	100	n.a. (∞)	1	1	9.49	28.7	0.98	1	1.09	-	-
#9 = #2 + #3 + #4 + #5	159	1	n.a	n.a	n.a	1	1	10.8	77.5	1	1		-	-

The ideal properties of the ground allow to operate the GHP also during the hottest months: $f_C = 0.7$ corresponds to the optimal capacity ratios for the actual air and ground temperatures. Energy consumption is slightly reduced and the corresponding ε value increases from 0.19 to 0.22.

In Configuration #3, the heating load is fully delivered by the GSHP, thanks to the enhanced heat transfer performance of the BHEs. However, in cooling mode, we deal with the same situation illustrated for Configuration #1; therefore, E_p^{tot} value does not decrease significantly.

In Configuration #4, the high performances of the ideal GHP allow to match the total building load. As in Configuration #1, $f_H = 0.9$ in January is due to the heat transfer effectiveness of the BHEs and to the constraints on $T_{w_{in}}$. The ε value reaches 0.42 and the primary energy consumption is notably reduced.

In Configuration #5, hydraulic head losses are neglected. Both N_{BHE} and $\dot{m}_w$ tend to infinity; thus, temperature alteration of the ground results negligible. The behavior is very similar to the one of Configuration #2: the small difference between the two E_p^{tot} values is due to the pumping energy.

In summary, for the first five configurations, where only the effect of single subsystems is investigated, the greatest improvement of the system performance is obtained by replacing the GHP unit with an ideal one (Configuration #4); on the contrary, the other components slightly affect the overall performance, even when loss-free.

The results of Configurations #6, #7, and #8 show that, when an ideal heat pump is present, it can be advantageous to improve the other subsystems, too. In Configurations #6 and #8, when an ideal heat pump is coupled with an ideal ground and with a system free of head losses, ε reaches, respectively, 0.74 and 0.75.

In conclusion, a technological development of GSHP components does not produce adequate benefits unless the efficiency of the heat pump unit is concurrently augmented. Conversely, the equivalence of ε values in Configurations #6 and #8 suggests that reducing both thermal and hydraulic losses of the heat pump is a possible way of obtaining high performances, even in the presence of a soil with unfavorable thermal properties.

6. Sensitivity analysis

In the previous section, it has been shown that the GHP is the key element for the improvement of the whole GSHP system. In this section, a sensitivity analysis is carried out on system performances, increasing the GHP second-law efficiencies in heating and cooling modes ($\eta_{H/C}^{II}$). The aim is to find a preferable path and practical upper limits for technological development of the heat pump device. $\eta_{H/C}^{II}$ is the ratio of actual COP/EER of the unit and the coefficient of performance of a theoretical loss-free heat pump, operating at the same temperatures of the sources (COP^*/EER^*).

$$\eta_H^{II} = \frac{COP}{COP^*} \qquad (4.1) \qquad\qquad \eta_C^{II} = \frac{EER}{EER^*} \qquad (4.2)$$

Optimal design and control strategies for minimum primary energy consumption are evaluated for different combinations of $\eta_{H,nom}^{II}$ and $\eta_{C,nom}^{II}$ values, starting from the nominal values and moving towards the ideal ones (see table 7).

Table 7. Nominal second-law efficiencies of GHP unit used for the sensitivity analysis (in parentheses, the efficiency increase with respect to the benchmark configuration).

$\eta_{H,nom}^{II}$	0.555[a]	0.6 (+8%)	0.7 (+26%)	0.8 (+44%)	0.9 (+62%)	1 (+80%)	
$\eta_{C,nom}^{II}$	0.397[a]	0.5 (+26 %)	0.6 (+51%)	0.7 (+76%)	0.8 (+102%)	0.9 (+127%)	1 (+152%)

[a] Current value (benchmark configuration) in rating conditions [24].

In every case, Minimum energy consumptions are obtained with 7 BHEs. The relative energy savings (percentage savings with respect to the benchmark value) are depicted in the contour plot of figure 1, as a function of second-law efficiencies in heating and cooling modes. A saturation trend can be observed for the system performance, which reaches its maximum (37% savings) for unitary values of $\eta^{II}_{H,nom}$ and $\eta^{II}_{C,nom}$.

The continuous red line represents the shortest path from the benchmark to the maximum, but its practical meaning is poor, as it is impossible to eliminate all the inefficiencies with a single technological leap. The dotted blue line, instead, is obtained by following the shortest paths between each consecutive iso-line (with steps of 5% savings) and shows a more realistic technological development strategy, based on step-by-step evolutions.

A practical indication that can be derived from the graph is that heating and cooling efficiencies should increase concurrently, but with a small, though significant, preference for heating mode improvement. This can be explained by the higher values of f_H with respect to f_C, with a greater weight associated to the heating performance.

It is worth recalling that – although the suggested development path and the outlined conclusions, strictly speaking, are valid only for the analyzed case study – the proposed method is generally applicable to any other building system, even selecting different objective functions.

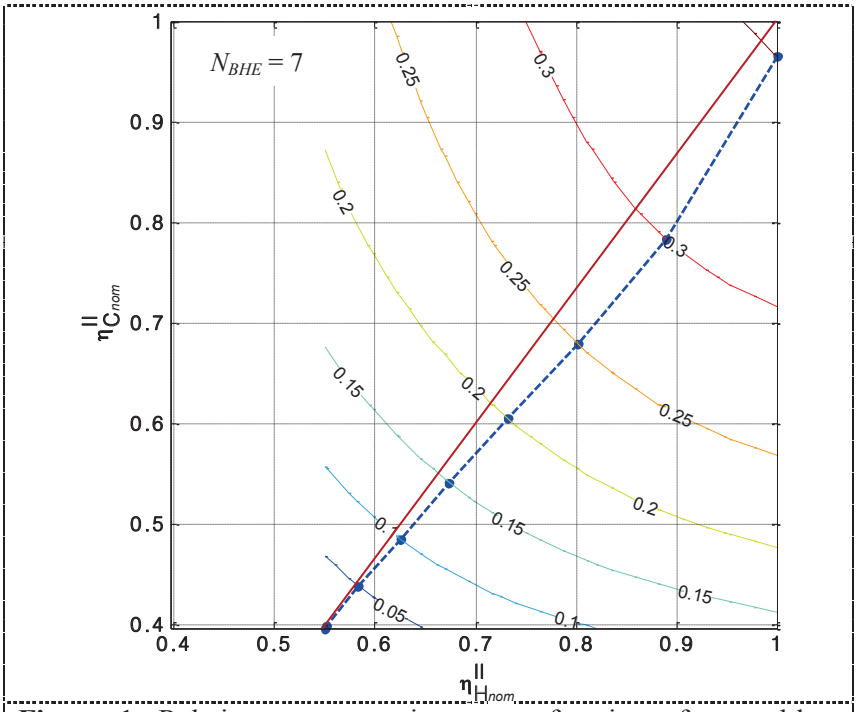

Figure 1. Relative energy savings as a function of second-law efficiencies in heating and cooling modes; the blue line follows the shortest path between two consecutive iso-lines.

7. Conclusions

In this work, the thermodynamic losses of a GSHP case study have been analyzed. Primary energy consumptions of nine configurations with different combinations of real and ideal subsystems have been compared, identifying their relative influence on the overall performance of the system. Furthermore, the use of theoretical loss-free components, together with optimized sizing and control strategies, allows to calculate the maximum energy savings achievable through the development of each subsystem.

The results reveal the possibility of an inherent hierarchical approach to the development of the subsystems. Specifically, the ground-coupled heat pump unit is the key element on which

technological development should be focused. Increasing GHP performances also allows to enhance the positive effects given by other components: e.g. the task efficiency is 42% in Configuration #4 (ideal heat pump unit) and 22% in Configuration #5 (no head losses); combining the two ideal subsystems (Configuration #8), ε reaches 0.75.

Focusing on the heat pump device, a sensitivity analysis is performed on its heating and cooling efficiencies, aimed at finding the best path of technological development. The results show a saturation trend of the system performance, but with different behaviors in heating and cooling modes, suggesting a small but significant preference for the promotion of the heating efficiency.

It has to be stressed that these conclusions do not have a general value, but depend on the particular case under exam. This notwithstanding, the proposed methodological approach can be applied to any other GSHP system (e.g. in other climatic conditions or on larger or smaller scale buildings).

As for future developments, they are mainly required for the hydraulic design of the evaporator/condenser and control capacity of the heat pump unit. The head losses in the evaporator/condenser have to be lowered through an optimized hydraulic design or with a proper layout of the ground-coupled loop. Besides, the penalization effects due to low capacity ratios should be reduced. To do this, the control range of the GHP unit should be as wide as possible or smaller capacity units should be installed, compatibly with the available economic budget.

This work deals only with energy savings. Economic and thermoeconomic aspects will be included in future works, in order to appropriately take into account in the optimization procedure also installation and technological development costs. In this way, a graph similar to the one of figure 1, but with iso-lines of thermoeconomic savings, should show a maximum, and the optimal way to reach it.

Nomenclature

Symbols and Acronyms

BHE	Borehole heat exchanger
c	Specific heat [J/(kg K]
COP	Coefficient of performance of the heat pump unit in heating mode
$CR_{H/C}$	Capacity ratio in heating/cooling mode
EER	Coefficient of performance of the heat pump unit in cooling mode
En_p	Primary energy consumption [MWh]
$f_{H/C}$	GSHP share of building load in heating/cooling mode
Fo_{BHE}	Fourier number at borehole surface
GHP	Ground-coupled heat pump unit
H	Borehole depth [m]
$\dot{m}$	Mass flow rate [kg/s]
N_{BHE}	Number of boreholes
$\dot{q}$	Heat flow per unit length [W/m]
Q	Thermal energy [MWh]
$\dot{Q}$	Thermal power [W]
R	Return function
R_b	Borehole thermal resistance [m K/W]
R_{BHE}	Borehole radius [m]
T	Temperature (K or °C)
$\mathbf{u}^n$	Vector of control variables
$\mathbf{U}$	Set containing all the u^n
$\mathbf{x}^n$	Vector of state variables

Greek Letters

α	Thermal diffusivity [m^2/s]
ε	Task efficiency (see equation 1)
η	Boiler efficiency
$\eta^{II}_{H/C}$	Second-law efficiency in heating/cooling mode
τ	Reference time scale [h]
ψ	Exergy efficiency

Subscripts

air	Air unit
bk	Back-up generator
C	Condenser
DC	Declared capacity
E	Evaporator
g	Ground
in	Inlet/supply
l	Building thermal load
nom	Nominal
out	Outlet/return
W	Water circulating in the ground-coupled loop

Superscripts

0	Initial time
*	Ideal conditions

References

[1] Bakirci K 2010 *Energy* **35** 3088–96
[2] Karabacak R, Güven Acar Ş, Kumsar H, Gökgöz A, Kaya M and Tülek Y 2011 *Int. J. Refrig.* **34** 454–65
[3] Montagud C, Corberán J M, Montero Á and Urchueguía J F 2011 *Energy Build.* **43** 3618–26
[4] Yu X, Wang R Z and Zhai X Q 2011 *Energy* **36** 1309–18
[5] Conti P, Grassi W and Testi D 2013 Proposal of a Holistic Design Procedure for Ground Source Heat Pump Systems *Proc. European Geothermal Congress 2013 (Pisa, IT)*
[6] Conti P, Grassi W and Testi D 2014 A Design Method for Ground Source Heat Pump Systems Based on Optimal Year-Round Performance - Part 1: Model Definition and Discussion *Submitt. to Appl. Energy*
[7] Conti P, Grassi W and Testi D 2014 A Design Method for Ground Source Heat Pump Systems Based on Optimal Year-Round Performance - Part 2: Conduction of a Case Study *Submitt. to Appl. Energy*
[8] Conti P, Grassi W and Testi D 2015 Proposal of Technical Guidelines for Optimal Design of Ground-Source Heat Pump Systems *Proc. World Geothermal Congress 2015 (Melbourne, AU)*
[9] Robert F and Gosselin L 2013 *Appl. Therm. Eng.* **61** 481–91
[10] Moran M J 1989 *Availability Analysis - A guide to efficient energy use (Corrected Edition)* ed ASME Press (New York: ASME Press)
[11] Bi Y, Wang X, Liu Y, Zhang H and Chen L 2009 *Appl. Energy* **86** 2560–5
[12] Lohani S P 2010 *Energy* **35** 3323–31
[13] Hepbasli A and Akdemir O 2004 *Energy Convers. Manag.* **45** 737–53
[14] Li R, Ooka R and Shukuya M 2014 *Energy Build.* **75** 447–55
[15] Ally M R, Munk J D, Baxter V D and Gehl A C 2013 *Int. J. Refrig.* **36** 1417–30
[16] Rosen M A and Dincer I 2004 *Int. J. Therm. Sci.* **43** 121–33
[17] Lohani S P and Schmidt D 2010 *Renew. Energy* **35** 1275–82
[18] UNI 2008 *UNI/TS 11300-2*
[19] UNI 2010 *UNI/TS 11300-3*
[20] UNI 2012 *UNI/TS 11300-4*
[21] Ingersoll L R, Zobel O J and Ingersoll A C 1954 *Heat conduction with engineering, geological and other applications* (New York: McGraw-Hill)
[22] Rao S S 1996 *Engineering Optimization: Theory and Practice* (Hoboken: John Wiley & Sons, Inc.)
[23] UNI 2012 *UNI 11466*
[24] UNI 2013 *UNI EN 14511-2*